contact us at:
journals@actapress.com or +1-403-288-1195.

Individual articles from the proceedings can also be purchased separately for **$25** each.

To place an order for Proceedings or individual articles, please visit the **ACTA Press Website**.

ACTA Press

A Scientific and Technical Publishing Company

Home · Login · My Cart · FAQ · Services · Caree

Proceedings

Prices are 40% off for all of 2002 to 2007 proceedings and have already been discounted 40% fro

Search or...

Select a Year: 2013 Search or...

Search By: Title Biomedical Engineering Search

Search: '**Biomedical Engineering**' in **Title**.
Sort: **Most Recent**
Proceedings Found: **10**

791: Biomedical Engineering 2013

Editor: A.R. Boccaccini
Location: Innsbruck, Austria
Publication Date: 27-Feb-2013
Hardcopy ISBN: 978-0-88986-953-0 ; **ISSN:** N/A
CD ISBN: 978-0-88986-942-4 ; **ISSN:** N/A
Online ISSN: N/A

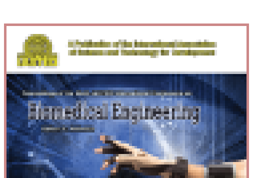

764: Biomedical Engineering / 765: Telehealth / 766: Assistive Technologi

Editor: C. Hellmich, M.H. Hamza, D. Simsik
Location: Innsbruck, Austria

Biomedical Engineering (BioMed 2013)

February 13 – 15, 2013
Innsbruck, Austria

Editor(s): A.R. Boccaccini

Other Years: 2013

Papers | Rates | Codes

Abstracts may contain minor errors and fomatting inconsistencies. Please contact us if you have any concerns or questions.

Add Checked Papers to Cart

Track	Biomedical Computing and Bioinformatics	Free	Subscription
791-031	**Classification of Ictal and Interictal EEG Signals** Zavid M. Parvez and Manoranjan Paul	Abstract	Buy now
791-061	**Automatic Snore and Breathing Sound Classification based on the Signal Envelope** Masato Kashihara, Takahiro Emoto, Udantha R. Abeyratne, Ikuji Kawata, Masatake Akutagawa, Shinsuke Konaka, and Yohsuke Kinouchi	Abstract	Buy now
791-090	**Rule Generation and Evaluation by Data Mining Ensembles for Clinical Decision Support** Simon Fong, Luke Lu, Kun Lan, Osama Mohammed, Jinan Fiaidhi, and Sabah Mohammed	Abstract	Buy now
791-093	**Four Phenotype Model of Interaction between Tumour Cells** Andrzej Swierniak, Michal Krzeslak, and Jaroslaw Smieja	Abstract	Buy now
791-092	**2-D Thresholding of the Connectivity Map Following the Multiple Sequence Alignments of Diverse Datasets** Tunca Doğan and Bilge Karaçalı	Abstract	Buy now
791-049	**A Novel Approach to Classify Human-Motion in Smart Phone using 2D-Projection Method** Yi Suk Kwon, Yeon Sik Noh, Ja Woong Yoon, Sung Bin Park, and Hyung Ro Yoon	Abstract	Buy now
791-068	**Evaluation of Blood Vessel Stiffness Index using Optical Recording with a Smart Phone** Chan-sol Yoon, Myeong-Heon Sim, Joo-Hong Chung, Sung Bin Park, and Hyung Ro Yoon	Abstract	Buy now
791-022	**Hybrid Filter for Removing Power-Supply Artifacts from EEG Signals** Alina Santillán-Guzmán, Ulrich Heute, Ulrich Stephani, Hiltrud Muhle, Andreas Galka, and Michael Siniatchkin	Abstract	Buy now
791-110	**Periodic Spatial Filter for Single Trial Classification of Event Related Brain Activity** Foad Ghaderi and Elsa Kirchner	Abstract	Buy now

Track	Measurement and Instrumentation	Free	Subscription
791-016	**A Simple Atrial Fibrillatory Wave Reconstruction Method for Frequency Analysis of Atrial Fibrillation using Single-Lead ECG** Xin Zhu, Daming Wei, Koji Fukuda, and Hiroaki Shimokawa	Abstract	Buy now
791-065	**A Four Channels Electrohysterograph with Individually Self Tuning Amplifier Gains** Wojciech M. Zabolotny, Agnieszka Podbielska, Wojciech Zaworski, Antoni Grzanka, and Dariusz Radomski	Abstract	Buy now
791-056	**A Fully Automatic Method for Accurate Parametrization and Reconstruction of ECG Waveforms** Emir Turajlic	Abstract	Buy now
791-136	**Evaluation of Three Mattress Designs for Capacitive ECG Measurement from Conductive Textiles on Bed** HongJi Lee, SeungMin Lee, and KwangSuk Park	Abstract	Buy now
791-064	**Instrumentation for Micromechanics Research in Trabecular Bone** Ondřej Jiroušek, Tomáš Doktor, Daniel Kytýř, and Petr Zlámal	Abstract	Buy now
791-039	**A Self-Tunable Dynamic Vibration Absorber for Tremor Suppression** Carlos J. Teixeira, Estela Bicho, Miguel F. Gago, and Luis A. Rocha	Abstract	Buy now
791-017	**Removing Artifacts from EEG Recorded within MR Scanner by Dynamical Template State Space Approach** Andreas Galka, Laith Hamid, Ulrich Stephani, and Michael Siniatchkin	Abstract	Buy now
791-142	**Recognizing Static and Dynamic Sitting Behavior by Means of Instrumented Office Chairs** Bernhard Schwartz, Andreas Schrempf, Kathrin Probst, Michael Haller, and Josef Glöckl	Abstract	Buy now
791-109	**Modeling and Resonant Attenuation of a Belt-Driven Cycling Device** Jyun-Ci Chen, Po-Wen Hsueh, and Mi-Ching Tsai	Abstract	Buy now
791-052	**A Gain Boosted Folded Cascode using Telescopic Boosting Amplifiers with Switched Capacitor Input Level Shifters** Bryce T. Bradford, Wolfgang Krautschneider, and Dietmar Schroeder	Abstract	Buy now
791-099	**A Low-Cost Microcontroller based Gas Flowmeter using a Specially Designed Parabolic Airway Resistor** Yekta Ülgen and Gulsah Kaçur	Abstract	Buy now
791-042	**Effect of Infrared LED Array Stimulation on EEG** Jih-Huah Wu, Wei Fang, Yi-Chia Shan, and Yang-Chyuan Chang	Abstract	Buy now

Track	Biomedical Signal Processing, Systems, and Control	Free	Subscription
791-102	**Application of Wavelet Transform to Analysis of Human Skin Blood Flux Signal** Tao Lei, Maogang Jiang, Yue Tian, Kangning Xie, Feijiang Li, Da Jing, Yili Yan, Guanghao Shen, and Erping Luo	Abstract	Buy now
791-158	**Cauchy Wavelet-based Mechanomyographic Analysis for Muscle Contraction Evoked by FES in a Spinal Cord Injured Person** Eddy Krueger, Eduardo M. Scheeren, André E. Lazzaretti, Guilherme N. Nogueira-Neto, Vera L.S.N. Button, and Percy Nohama	Abstract	Buy now
791-069	**Automatic Evaluation of Gastrointestinal Motor Activity through the Analysis of Bowel Sounds** Koichi Shono, Takahiro Emoto, Toshiya Okahisa, Udantha R. Abeyratne, Hiromi Yano, Masatake Akutagawa, Shinsuke Konaka, and Yohsuke Kinouchi	Abstract	Buy now
791-149	**Computer Models for Gait Identification and Analysis using Autonomous System for Control and Monitoring** Ivanka P. Veneva	Abstract	Buy now
791-083	**A Study of Temporal Structure of Glottal Flow Derivative Estimates Associated with Laryngeal Pathology** Emir Turajlic and Dzenan Softic	Abstract	Buy now
791-126	**Knowledge Discovery and Knowledge Reuse in Clinical Information Systems** Jon D. Patrick, Leila Safari, and Yuzhong Cheng	Abstract	Buy now
791-174	**Wavelet Filter Proposal to Attenuate the Background Activity and High Frequencies in EEG Signals** Geovani R. Scolaro, Christine F. Boos, and Fernando M. Azevedo	Abstract	Buy now
791-156	**Automated Extraction of Principal Components of Non-Structural Protein 1 from SERS Spectrum** Afaf R. Mohd Radzol, Yoot K. Lee, Wahidah Mansor, and Faizal Mohd Twon Tawi	Abstract	Buy now
791-144	**Classification of Photoplethysmographic Signals using Support Vector Machines for Vascular Risk Assessment** Rohan Baid, Niranjana Krupa, and Muhammad A.M. Ali	Abstract	Buy now
791-159	**Changes in Bilateral Phase Synchronization in Parkinsonian Tremor Related to Amplitude Difference** Sang Kyong Kim, Hyo Seon Jeon, Han Byul Kim, Ko Keun Kim, Beom Seok Jeon, and KwangSuk Park	Abstract	Buy now
791-082	**Robotic Arm Control with Brain Computer Interface using P300 and SSVEP** Ozan Çağlayan and Reis Burak Arslan	Abstract	Buy now
791-134	**Speech Training System for Thai Therapeutic Robot** Orrawan Kumdee, Siriwan Chumpiya, Chetthana Ruangjirakit, and Panrasee Ritthipravat	Abstract	Buy now
791-141	**An Electro-Mechanical Contact Formulation for Dry/Wet Electrode-Scalp Interfaces in an EEG Headset** Vangu Kitoko, Tuan N. Nguyen, and Hung T. Nguyen	Abstract	Buy now
791-138	**A Population Search Algorithm for Clustered Multivariate Solutions: Application to EEG Connectivity** Ian Daly, Reinhold Scherer, and Gernot Müller-Putz	Abstract	Buy now
791-094	**Recovering Vital Physiological Signals from Ambulatory Devices** Praveen Pankajakshan and Rangavittal Narayanan	Abstract	Buy now
791-100	**A Time-Series Pre-Processing Methodology for Biosignal Classification using Statistical Feature Extraction** Simon Fong, Kun Lan, Paul Sun, Sabah Mohammed, and Jinan Fiaidhi	Abstract	Buy now
791-077	**Wrist Pulse Signal Acquisition System Design** Bhaskar Thakkar and Anoop L. Vyas	Abstract	Buy now
791-112	**Haematoma Detection using EIT in a Sheep Model** Seyedeh Bentolhoda Ayati, Kaddour Bouazza-Marouf, David Kerr, and Michael O'Toole	Abstract	Buy now

Proceedings of the IASTED International Conference
Biomedical Engineering (BioMed 2013)
February 13 - 15, 2013 Innsbruck, Austria

AN ELECTRO-MECHANICAL CONTACT FORMULATION FOR DRY/WET ELECTRODE-SCALP INTERFACES IN AN EEG HEADSET

Vangu Kitoko, Tuan N. Nguyen and Hung T. Nguyen, *Senior Member, IEEE*
Centre for Health Technologies, Faculty of Engineering and Information Technology, University of Technology Sydney, NSW 2007 – Australia
(Vangu.Kitoko@student.uts.edu.au)

ABSTRACT
The process of generating an initial prototype for a new dry electrode wearable EEG headset system design can be time and resource intensive. The ability to predict the mechanical and electrical characteristics of this recording device could lead to major cost savings in this process. Since the skin surface roughness has a deep impact on the decrease of brain electric contact conductance (or the increase of the contact impedance) when electrode with bristles contact scalp skin, the estimation of electric conductance across rough dry and wet boundaries is a challenging task in the designing optimization of the wearable EEG headset system. In this contribution, the contact mechanism to predict the electrical impedance of scalp skin pressed against the electrode is considered as the electrical connection by the mechanical contact. With this, we have extended the Pohrt and Popov model by including the effects of conductive gel. An experiment is developed and carried-out to validate the interfacial contact impedance model.

KEY WORDS
Bristle electrode, Wearable EEG headset, Skin roughness, scalp, loading pressure, contact impedance, optimization.

1. INTRODUCTION

When an electrode's bristles and scalp skin are squeezed into contact, brain electrical activities of a few microvolts (5 to 100 μV), called EEG signals, are passed from the skin to the electrode [1, 2]. As the electrode's bristles and scalp skin surfaces are pressed together, the skin's soft surface is squashed flat elastically by the contact pressure, so that perfect or full smooth contact is observed by the naked eye through the nominal contact area A_0. In reality, the perfect contact never exists, skin micro-scale surfaces, no matter how carefully prepared, always contain surface roughness (hills and valleys) or deviations which are largely compared to an atomic-size and are often called surface asperities [3, 4]. The roughness on the skin surface causes the contact to be restricted to a set of micro-contact spots, randomly distributed on the apparent contact area. The sum of all these areas constitutes the real (true) area of contact, A_r, which is a small fraction of apparent or nominal area A_0 [5, 6].

If we now conduct the brain electrical transfer as function of applied pressure from the scalp skin to the electrode's headset, the ion current from the brain is restricted to flow through the micro-contact spots. Constriction of the electrical current by spots reduces the volume of material used for electrical conduction, significantly decreasing the expected contact conductance or increasing the contact impedance beyond the case of a fully conducting contact area [5]. In the case of this study, the contact conductance between electrode and skin must be increased (or decreased the contact impedance) as much as possible in order to avoid artifacts and record better quality brain signals.

The importance of the prediction of the electrical contact conductance as function of applied pressure has been clearly recognised since the earliest studies on contact mechanics [7, 8]. Contact mechanics modelling of this kind has focused on lightly loaded rigid solid contact interface. However, for a soft solid having a randomly rough surface (like skin) pressed against a flat rigid solid, the mechanical analysis for self-affine using the finite element method (FEM) has contributed to identifying the real contact area [9, 10] and stiffness change of the contact [11, 12], which can be interpreted in terms of contact conductance as a function of the applied load F_N [13, 14].

In this contribution, the prediction of electrode-scalp electrical contact conductance (or contact impedance) is examined. For simplification, the contact mechanism of scalp skin pressed against the electrode is considered as the electrical connection by the mechanical contact. Thus, in order to predict contact conductance, the interfacial contact is separated into two parts: mechanical contact and electrical connection. For mechanical contact analysis, a new normal force-displacement approach based on the micro-mechanical studies is developed for analyse of the non-linear electrode-skin contact interface problem with "high contact precision". Finite element method (FEM) was well used to account for the geometry of the device and for predicting the interfacial non-uniform pressure distribution when the headset-electrodes block is pressed on the skin scalp under a constant loading pressure.

For the electrical contact conductance modelling, this work adopts the models presented in [15] to predict the interfacial normal contact stiffness and contact conductance when the dry electrode is pressed on the scalp skin. After the dry contact calculation, conductive gel (paste) with a given thickness is introduced to cover the deformed rough surface and improve the conductance. In this paper, we have extended the Pohrt and Popov model [15] by including the effects of conductive gel.

DOI: 10.2316/P.2013.791-141

This approach provides a means to gain insight on the effects of conductive gel when a wet electrode is pressed on the scalp skin.

2. METHODOLOGY

2.1 Wearable Headset

In a more generalised view, a wearable EEG headset (Figure 1) can be defined as a sub-system (or front-end interface) that records and delivers a vital brain signal to a higher level application or overall EEG system. The functioning block diagram of the wearable headset, shown in Figure 2, consists of three parts: electrodes for signal acquisition, signal amplification and wireless transmission / receiving for data transmission.

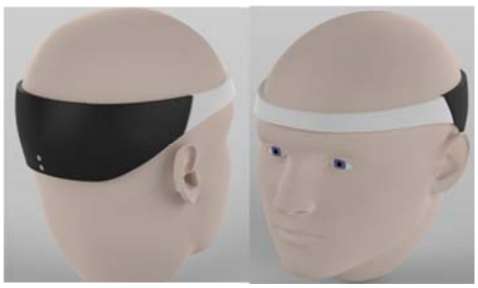

Figure 1: The prototype wireless headset system

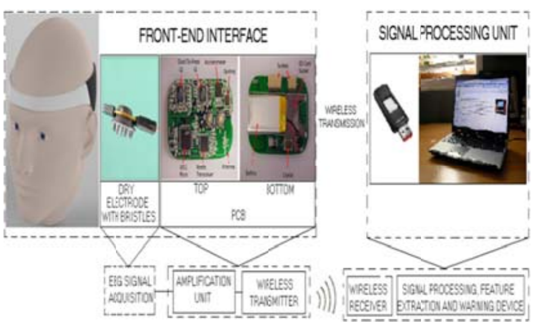

Figure 2: Block diagram of a wireless EEG system in development.

In the case of this work, the headset is incorporated with a number of dry and wet electrodes with bristles, placed in accord with the targeting EEG recording regions (see Figure 3).

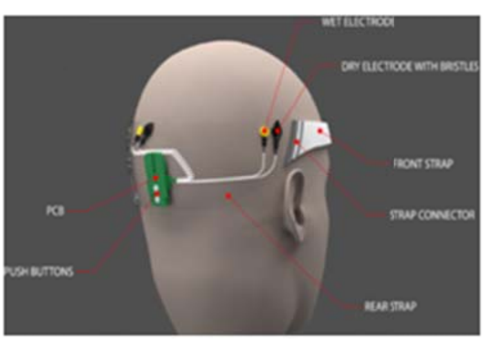

Figure 3: Electrode placements

Two dry electrodes are mounted on the targeted region of the headset in accord with the 10/20 electrode placement system as follows: the bristle-electrode for data recording was placed over the left occipital region (O1) and its reference electrode also was a bristle-electrode placed at T4 [1]. All electronics components are integrated on-board a printed circuits board (PCB) which was designed in miniature to serve as a sensing module and improve the headset hardware flexibility. The PCB and part of the electrode, except the bristles, are internally fixed in the headset.

2.2 Electrode with Bristles

This electrode is reusable silver/silver chloride made with twelve 2 mm contact posts or bristles for EEG testing without the need for scalp preparation and use of conductive gel or paste (Figure 4A).

Figure 4: (A) Electrode with bristles and (B) Bristle electrode with clip lead.

So, when the headset is appropriately pressed on the scalp skin and held firmly in contact, the bristles will penetrate thick hair, press into the skin without penetrating beyond the epidermis and providing a quick and efficient electrical contact between the electrode and the scalp.

2.3 Contact Mechanics Formulation

2.3.1 Macroscopic Model

Contact between the wearable headset and scalp skin can be modeled simply by using the basic unilateral contact law by referring to the Kuhn-Tucker-Karush or Signorini conditions [16]. This is completely described by the following set of inequalities and the nonlinear complementarily relation,

$$g_N \geq 0 \qquad p \geq 0 \qquad p g_N = 0 \qquad (1)$$

In this formulation, the essence of the contact problem lies in the fact that any point on the boundary of each body must either be in contact or not in contact. If it is not in contact, the gap g_N between it and the other body must be positive $(g_N > 0)$ whereas if it is in contact, $g_N = 0$, by definition. A dual relation involves the contact pressure p between the bodies which must be positive

$(p > 0)$ where there is contact and zero $(p = 0)$ where there is no contact.

The relation (1) provides the basis to treat electrode-skin contact as a non-penetration problem, but with "low contact precision", where the most essential necessity is the correct enforcement or optimisation of the headset geometry. However, due to the extremely complex structure of the skin roughness surface, the chemical and the physical behaviour of the material close to the interface (conductive gel, skin or electrode metal), analysis of the electrode-skin contact interface problem requires "high contact precision". To do so, we will consider effects related to the micro-mechanical contacting surfaces which have to be solved on a macro-scale level.

2.3.2 Microscopic Model

For the purpose of this analysis let us consider the block headset-electrode, as a flat rigid surface, pressed against the scalp, as rough soft surface, at a constant loading pressure σ_0 around the headset (Figure 5). Each electrode is a metal with elastic modulus $E_{el} = E$, a flat surface or area A_0 and a thickness d.

We will study both wet and dry interfaces, resulting with and without the presence of conductive gel at the electrode-skin wall interface. When flat and rough surfaces are brought into dry contact they touch initially at a single point or along a line. Under the action of the slightest load, electrode-headset block is squeezed against a soft, randomly rough surface.

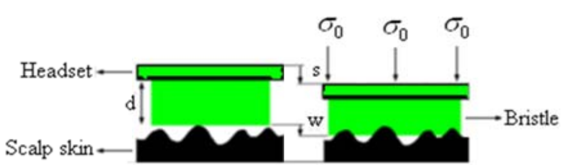

Figure 5. An headset-electrode's bristle block in wet contact with a soft, randomly rough skin. Left: no applied load. Right: the block is squeezed against the skin with normal loading force $F_N = \sigma_0 A_0$.

The rough solid deforms in the vicinity of its point of first contact so that both bodies touch over an area which is finite though small compared with the dimensions of the two bodies. The upper surface of the bristle-headset will move downwards by the distance s, which is the sum of a uniform compression of the bristle-headset block, $d\sigma/E$, and a movement or penetration w of the average position of the lower surface of the bristle into the valleys or cavities of the skin counter surface:

$$s = w + d\frac{\sigma}{E} \qquad (2)$$

Let us now denote the separation between the average surface plane of the flat hard solid and the average surface plane of the rough soft solid by u with $u \geq 0$. Since for low squeezing pressure, the area of real contact A_r varies linearly with the squeezing force $F_N = \sigma(u)A_0$, Lorenz et al. [13] found that an exponential rise in load with decreasing u,

$$F_N = \beta A_0 E^* e^{-u/u_0} \qquad (3)$$

where $u_0 = \gamma h_{rms}$ and h_{rms} is the root mean square (rms) variation in surface height; where γ is a constant of order 1 and β is a characteristic which depends on the surface roughness but is independent of the pressure σ [17]. Since we assume only electrode material is much more elastic than the skin, the effective (called also harmonic or contact) elastic modulus E^* is just the plane-strain modulus $E^* = E_{el}/(1-\nu_{el}^2) \approx 4E_{el}/3$ as for bristle $\nu_{el} \approx 0.5$ [17, 18]. Using (3) gives

$$\log\left(\frac{\sigma}{E_{el}}\right) = B + \frac{1}{u_0}\left(s - d\frac{\sigma}{E_{el}}\right) \qquad (4)$$

where $B = \log(4\beta/3) - h_{max}/u_0$, $\sigma = F_N/A_0$ is the squeezing pressure and $E_{el} = E$ and ν_{el} are the elastic moduli and the Poisson ratio for the electrode, respectively.

The equation (4) is exact whenever the contact between the electrode block and the rough soft is dry, no conductive gel film is used at the interface. For wet contact boundary conditions, this takes the form

$$\log\left(\frac{\sigma}{E'}\right) = B' + \frac{1}{u_0}\left(s - d\frac{\sigma}{E'}\right) \qquad (5)$$

where the elastic modulus for wet contact interface $E' > E$ is consistent with the prediction of the Lindley equation [19]. Equations (4) and (5) predict that for small squeezing load F_N, the interfacial separation u depends logarithmically on F_N [20]. These equations are mechanically non-linear.

2.3.3 Finite Element Method

The finite element method is well suited to account for the geometry of the device and for the non-uniform mechanical of the contact interface. By applying the FEM to the headset-scalp, numerical simulations are performed for the scalp targeted region, considered as a rough elastic surface in contact with bristles, as perfectly rigid flat surfaces, in order to find the contact distribution. To perform this analysis, we use an adaptative FEM simulation package, SolidWorks simulation. The properties of both materials used by FEM are shown in Table I [9].

Table I
Parameters for normal contact simulation

Parameter	Skin	Electrode
Young's modulus	0.3 MPa	20 GPa
Poisson's ratio	0.459	0.4
Electrical resistivity [10^{-8} Ω/m]	100000	1.7

Periodic boundary conditions are imposed at the contact surfaces to eliminate boundary effects and a contact algorithm is used only to enforce the impenetrability constraint on the two surfaces.

Results

The sample results of FEM analysis are as follows. Figure 7 shows the distribution of contact pressure due to different displacements determined when a constant loading pressure is applied around the headset. It is observed that the pressure distribution of the headset contacting with the occipital region of the scalp (where recording electrodes are placed [1]) is larger compared to that in others regions. This is related to the increased deformation or displacement imposed by the presence of electrodes.

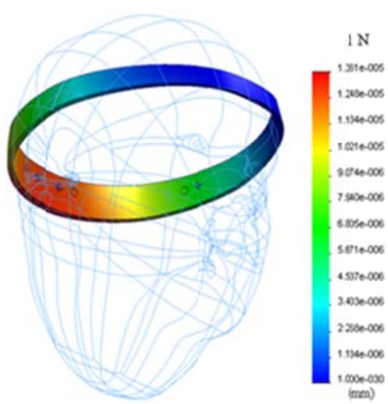

Figure 7. Contact pressure distribution at various displacement between headset and scalp at 1 N/m using the FEM simulation with bristle's normal shape.

2.4 Interfacial Electrical Contact Conductance Formulation

2.4.1 Dry Contact Interface

The mechanical analysis presented using a computer-generated self-affine surface FEM has contributed to identifying the normal contact stiffness change which will contribute to determine the electrical contact conductance model. Based on the analogy presented by Barber in [21], this work considers the dimensionless analytical expression for the contact conductance $\left(C_{dry}\right)$, presented by Pohrt and Popov [15], to analyse the normal contact between skin rough self-affine surface and the electrode's flat rigid body in dry conditions. Thus,

$$C_{dry} = \frac{1}{Z_{dry}} = \frac{\pi D_f \sqrt{A_0}}{5\left(\rho_{flat} + \rho_{rough}\right)} \left(\frac{F_N}{E^* h \sqrt{A_0}}\right)^{0.2567 D_f} \quad (6)$$

where Z_{dry} is the specific interfacial contact impedance. Where E^* and $\rho = \rho_{flat} + \rho_{rough}$ are the combined Young's elastic modulus and the combined resistivities of the two contacting bodies, respectively. The relation (6) is valid only for dry contact interface. For wet contact interface this equation no longer holds due to the presence of conductive gel between electrode and skin. This work therefore extends the Eq. (6) to estimate the contact conductance or impedance in wet conditions by including a parameter in the normal stiffness representing the presence of conductive gel at the interfacial contact between the electrode's bristles and the scalp skin.

2.4.2 Wet Contact Interface

It is known that when a flat electrode surface comes in static contact on the scalp skin rough surface, the contact is not directly in equilibrium [22]. With the presence of conductive gel (paste), two actions occur before the interface reaches equilibrium. First, curved menisci form around the contacting and near contacting spots due to gel mediated adhesion on the skin surface [22-25]. Besides the meniscus, the ions in the gel are rapidly filled-up into the skin by diffusion due to the existing concentration gradient [22], thus ensuring a maximum electrical conductivity (or a minimal electrical impedance) in the wetted areas.

Based on the Young and Laplace equation and assuming that the liquid film thickness is uniform everywhere on the flat surface, the meniscus force (also referred to as adhesive force), F_m, is then numerically calculated using the extended first principle of the micro meniscus theory [26] by the following equation:

$$F_m \approx \frac{\gamma_L \left(\cos\theta_1 + \cos\theta_2\right) A_m}{h_m} \quad (7)$$

where θ_1 and θ_2 are the contact angles of the liquid on the two solid surfaces, h_m is the mean meniscus height, and γ_L is the surface tension of the liquid and where A_m is the total projected meniscus area.

With an additional meniscus force existing at the contact interface, the total normal force on the wetted interface F_N^W is the externally applied normal force F_N plus the additional meniscus force F_m

$$F_N^W = F_N + F_m \quad (8)$$

Thus, we can directly obtain an approximate expression for the wet contact conductance by substituting (8) for (6).

$$C_{wet} = \frac{1}{Z_{wet}} = \frac{\pi D_f \sqrt{A_o}}{5\left(\rho_{flat} + \rho_{rough} + \rho_{gel}\right)} \left(\frac{F_N + F_m}{E^* h \sqrt{A_o}} \right)^{0.2567 D_f} \quad (9)$$

where Z_{wet} and ρ_{gel} are the contact impedance and the resistivity for conductive gel, respectively.

3. EXPERIMENT

To validate the interfacial contact impendance model, we have performed experimental investigations when the wearable headset is squeezed on the scalp skin in dry and wet conditions as illustrated in Figure 3. The experiment was undertaken at the Centre for Health Technologies (CHT) with the understanding and written consent of each participant, following the recommendations of the ethics committee of the University of Technology, Sydney-Australia.

The principle of the experimental test rests in the comparison of the different pressing loads at the electrode-scalp contact interface to having different contact impedance. To carry out these tests, we collected data from ten (10) healthy subjects (7 males including 2 dark-skinned and 5 fair-skinned, and 3 females including 1 dark-skinned and 2 fair-skinned). This is because we have noted that the skin impedance differs from person to person [15]. All of the measurements were performed while the subjects were sitting and all participants were volunteers.

To measure the interfacial contact impedance, the Siesta system was intended for use in the displaying, monitoring, recording, printing and storage of the contact impedance of each electrode-scalp involved and signal calibration features. We measured the impedance Z over the squeezing load F_N for two different cases: dry and wet. First the dry bristle electrode was used, without gel or pasta. Second, we used Ten20 Conductive gel (D.O. Weaver and Co, Aurora-USA) to wet the electrode's bristle contact areas. Because of its high viscosity, the fluid is an excellent lubricant; hence it was not easily squeezed out of the contact area under normal pressure applications.

To measure the contact pressure at the electrode-skin scalp contact interface, we used a sub-miniature load cell (Models LPM 500–COOPER Instruments), in combination with a manual inflation head pressure cuff (Omron-Australia) as a pressure pad. The pad is placed directly on top of the headset worn on the subject's scalp and held in place with an adjustable section for bespoke fit (Velcro). The loading force F_N was changed in steps of 0.1 by inflating the pad from the bulb. Thus, the contact pressure could be varied and the interfacial impedance was measured. The data was sent from the data acquisition system over a serial connection and processed on a PC using Profusion PSG 2 software for reviewing, analysing, processing and validation.

Figure 9: Manual inflation head pressure cuff and the load cell.

3.1 Results

The contact impedance obtained using dry and wet contact interface are plotted against the contact load in figure 10, when compared with that of the simulation theory of wet interface as given in equation (9). The compared interfacial contact impedances results exhibit a converging behaviour when a low squeezing pressure range is applied. They decrease rapidly at a small squeezing load and then decrease gradually as the load is increasing. In addition, results obtained using wet contact interfaces (Bristles and Gold electrodes) are closer to that of Pohrt's analogy than with dry contact conditions.

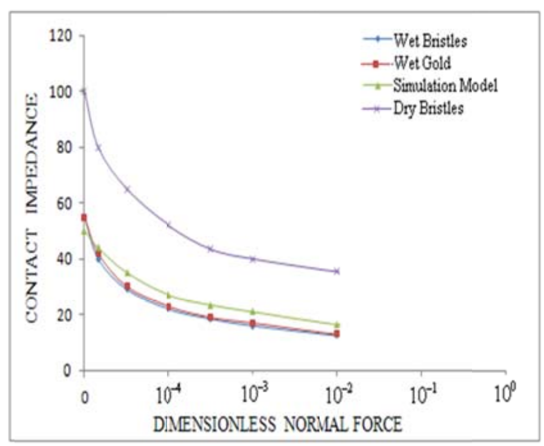

Figure 10: Dimensional interfacial impedance obtained using dry and wet (bristles and Gold) contact interface plotted against the contact load, when compared with simulation equation of Pohrt and Popov [15].

3.2 Optimization of the Contact Pressure Distribution

In the context of EEG recording applications, the contact impedance between skin-electrodes must be decreased as much as possible in order to maintain better quality recording signals [1, 22, 27]. Hence, an optimum skin-electrode real contact shape producing minimum interfacial contact impedance is expected in the headset designing. However, it is difficult to exactly optimise contact shape directly. The first question is what a contact pressure distribution (p_n) gives minimum contact impedance (Z) when the total compression force (F) is fixed. The optimum problem can therefore be described as follows:

Find $\quad p_n(x) \quad$ (10)

Minimum $\quad Z = Z(p_n)$

When $\quad \int_0^l p_n \mathrm{d}x = F \quad$ are given.

The design variable is the contact pressure distribution, and the objective function, i.e., contact impedance, which is a function of contact pressure distribution [28]. The optimisation process shows that a constant pressure distribution is therefore an optimum pressure distribution:

$$p(x) = \frac{F}{L} \tag{11}$$

where L is the perimeter of the contact region.

From this optimization analysis, we have measured the estimating optimal contact impedance when bristles are pressed on the scalp with increasing loads for the case where one contact surface is wet (bristles and gold) and the other dry. Ten tests were performed on five different subjects studied. All of the measurements were performed while the subjects were sitting. The contact pressure at the interface was increased gradually to assess its influence on the interfacial scalp-skin impedance and at the same time to insure subject comfort. The contact impedances obtained with increasing loading pressure are plotted in Figure 11.

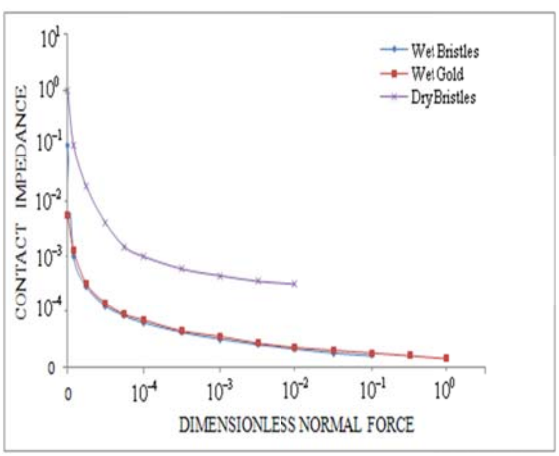

Figure 11: The contact impedances at optimal loading pressure

The optimum loading was determined as a sign of subject discomfort (pain). While using dry bristles, all participants studied displayed discomfort (pain) when the increased pressure reach dimensionless values of 10^{-2} or higher. At the same time, with the presence of the viscous paste on the contact interface, we were able to gradually increase pressure up to 10^{-1} (ten times higher) for wet bristles condition and up to 10^{0} (hundred times higher) for the gold wet condition, no signal of discomfort has been registered from participants.

3.3 EEG Recording

Besides the contact impedance evaluation, we compare the performance of the wet and dry bristle electrodes in recording EEG data with the standard wet gold-plated cup electrode using a 2 channel recording device, as shown in figure 3. For this end, five participating subjects performed two mental tasks, eyes-closed and arithmetic calculation. Since only two mental tasks were required to be classified, one electrode located in O_1 position was used to collect EEG signals during the mental task performing procedure. Eyes-closed command data were collected from each of 5 participants for a period of 20sec and the same procedure was applied for the mathematical calculation task. These data were used for both statistical and classification analyses.

As a result, power spectra were presented for wet and dry bristle electrodes in comparison with wet gold electrode (Figure 12).

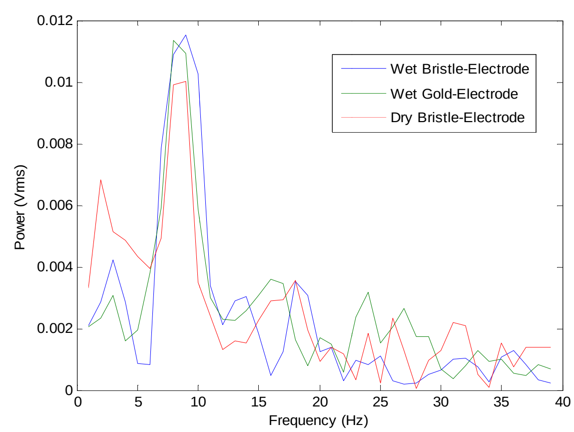

Figure 12: EEG activity recorded with wet and dry bristle electrode in comparison with gold electrode for eyes-closed task at loading pressure of $0.5N$.

Although, all three electrode recordings have shown prominent peaks in the alpha frequency band around $10Hz$ and also in the beta range $(15-25Hz)$, around $20Hz$, but, with the presence of loading pressure at the contact interface, the dry bristle electrode did reveal less increasing compared with the two other wet electrodes.

3.4 Electrode Classification

For optimal robustness of the evaluation, the classification approach with brain-computer interface (BCI) was performed with both wet and dry electrode with bristles using two mental tasks: eyes-closed and mathematical calculation, as presented in figure 13. This aimed at showing the possibility of performing the BCI experiment with the electrode with bristles and not at comparing them with wet gold electrode.

The combined EEG raw data were first transformed in FFT domain and the EEG powers at frequencies from 1 to 40Hz were then fed into Matlab-Multilayer Feed-Forward Neural Network. By trial and error, 30 hidden nodes were chosen, and only one output node was required for two-task classification (0 for arithmetic calculation task and 1 for eyes-closed task).

For two-mental task classification, the overall accuracy of a neural network trained with EEG data collecting from wet bristle electrodes was 98.79%, whereas the accuracy of a neural network trained with EEG data collecting by dry bristle electrode was 93.17%. This difference is mainly due to some instability behaviour observed in recording EEG data when the dry bristle electrode is pressed on the scalp compared with the wet one.

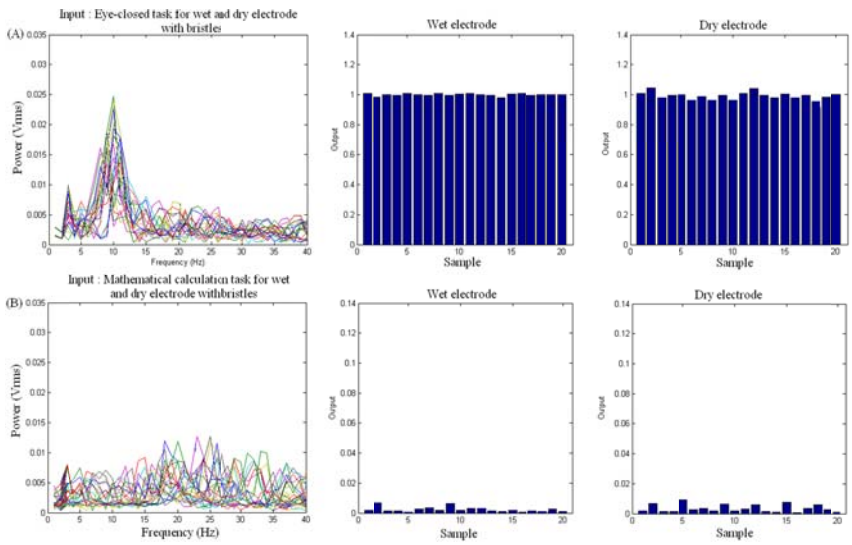

Figure 13: Eyes-closed and mathematical calculation mental tasks using wet and dry electrode with bristles at loading pressure of 0.5N.

4. SUMMARY AND CONCLUSION

The results of this study can be summarised as follows:

- The micro-mechanical contact model developed and analysed using a computer-generated self-affine surface FEM has contributed to evaluate the contact pressure distribution between headset-electrode block and scalp.
- The presence of this distributed pressure results in the normal contact stiffness change which has contributed to determine the electrode-scalp interfacial electrical contact conductance (or impedance) models for dry and wet bristle-scalp contact interface.
- Although the compared interfacial contact impedances results exhibit a converging behaviour when a low squeezing pressure range is applied, results obtained using wet contact interfaces (bristles and gold electrodes) are closer to that of the simulation model than with dry contact conditions.
- From the optimization analysis, the contact pressure at the interface was increased gradually to assess its influence on the interfacial scalp-skin impedance and at the same time to insure subject comfort. Thus, the optimum loading value for each case studied was determined as a sign of subject discomfort (pain).
- For optimal robustness of the evaluation, the classification approach with a brain-computer interface (BCI) was performed with both wet and dry electrodes with bristles. For the two-mental task classification, the overall accuracy of the Neural Network trained with EEG data collecting from wet bristle electrodes was higher and stable when compared with dry bristle electrodes pressed on the scalp at the same loading pressure.
- We conclude this paper by pointing out that the dry bristle electrode can be used in recording EEG only when minimal scalp-electrode contact pressure is required to obtain a robust mechanical fixation. However, when the increased loading pressure is needed prior to obtaining better EEG signal quality, dry electrodes are not adequate for use when avoiding subject discomfort or penetrating the scalp.
- This would suggest the optimisation of the perimeter or lateral contact surface of each bristle in the electrode, to maximising the displacement and then the area of real contact between bristles in the electrode and the target region of scalp-skin.

ACKNOWLEDGEMENTS

Authors thank Dr Phuoc Huynh (School of Electrical, Mechanical and Mechatronic Systems-University of Technology Sydney) and Nicholas Karlovasitis (Director, Design-By-Them – Australia) for their kindly supports and usefully contributions.

REFERENCES

[1] V. Kitoko, T. N. Nguyen, J. S. Nguyen, Y. Tran, and H. T. Nguyen, "Performance of dry electrode with bristles in recording EEG rhythms across brain state changes," *IEEE EMBS Boston, USA, August 30 - September 3,* 2011.

[2] H. Nguyen, "Electroencephalogram," in *Biomedical Instrumentation and applications*, ed: University of Technology, Sydney - Australia, 2008.

[3] C. Flynn, A. Taberner, and P. Nielsen, "Measurement of the force-displacement response of in vivo human skin under a rich set of deformations," *Medical Engineering & Physics,* vol. 33, pp. 610-619, 2011.

[4] F. M. Hendriks, D. Brokken, J. T. W. M. van Eemeren, C. W. J. Oomens, F. P. T. Baaijens, and J. B. A. M. Horsten, "A Numerical-experimental method to characterize the non-linear mechanical behaviour of human skin," *Skin Research and Technology,* vol. 9, pp. 274-283, 2003.

[5] R. S. Timsit, "Electrical Contact Resistance: Properties of Stationary Interfaces," *IEEE Transactions on Components and Packaging technologies,* vol. 22, pp. 85-98, 1999.

[6] F. P. Bowden and J. B. P. Williamson, "Electrical conduction in solids. I: Influence of the passage of current on the contact between solids," *Proceedings of the Royal Society of London. A: Mathematical and Physical Sciences,* vol. 246 (1244), pp. 1-12, 1958.

[7] J. A. Greenwood, "Constriction resistance and the real area of contact," *British Journal of Applied Physics,* vol. 17, pp. 1621-1632, 1966.

[8] R. Holm, *Electrical contacts handbook, Springer*, 1958.

[9] S. Hyun, L. Pei, J. F. Molinari, and M. O. Robbins, "Finite element analysis of contact between elastic self-affine surfaces," *Phys.Rev. E70-026117. DOI : 10.113,* 2004.

[10] M. Borri-Brunetto, B. Chiaia, and M. Ciavarella, "Incipients liding of rough surfaces in contact: a multiscale numerical analysis," *Comput. Methods Appl. Mech. Eng,* vol. 190, pp. 6053-6073, 2001.

[11] C. Campana, B. N. J. Persson, and M. H. Muser, "Transverse and Normal Interface Stiffness of Solids with Randomly Rough Surfaces," *Journal of physics: Condens. Matter* vol. 23, p. 085001 (9 pages), 2011.

[12] L. Pei, S. Hyun, J. F. Molinari, and M. O. Robbins, "Finite element modeling of elasto-plastic contact between rough surfaces," *J. Mech. Phys. Solids,* vol. 53, pp. 2385–2409, 2005.

[13] B. Lorenz, G. Carbone, and C. Schulze, "Average separation between a rough surface and rubber block: Comparison between theories and experiments," *Wear,* vol. 268, pp. 984-990, 2010.

[14] D. P. Boso, G. Zavarise, and B. A. Schrefler, "A Formulation for electrostatic-mechanical contact and its numerical solution," *International Journal For Numerical Methods In Engineering,* vol. 64, pp. 382-400, 2005.

[15] R. Pohrt and V. L. Popov, "Normal Contact Stiffness of Elastic Solids with Fractal Rough Surfaces," *Physical Review Letters,* vol. 108, p. 104301 (4 pages), 2012.

[16] P. Wriggers and J. Nettingsmeier, "Homogenization and Multi-scale Approaches for Contact Problems," in *Computational Contact Mechanics: CISM Courses and Lectures No: 498*, P. Wriggers and T. A. Laursen, Eds., ed Springer Wien-New York, pp. 129-161, 2007.

[17] B. N. J. Persson, "Contact mechanics for randomly rough surfaces," *Surf. Sci. Rep,* vol. 61, p. 201, 2006.

[18] K. L. Johnson, *Contact mechanics. Cambridge University Press, Cambridge*, 1985.

[19] B. Lorenz, G. Carbone, and C. Schulze, "Average separation between a rough surface and a rubber block: Comparison between theories and experiments " *Wear,* vol. 268, pp. 984-990, 2010.

[20] B. N. J. Persson, O. Albohr, U. Tartaglino, A. I. Volokitin, and E. Tosatti, "On the nature of surface roughness with application to contact mechanics, sealing, rubber friction and adhesion," *Journal of Physics: Condens. Matter,* vol. 17, pp. R1-R62, 2005.

[21] M. Paggi and J. R. Barber, "Contact conductance of rough surfaces composed of modified RMD patches," *International Journal of Heat and Mass Transfer,* vol. 54, pp. 4664-4672, 2011.

[22] E. McAdams, "Bioelectrodes," in *Encyclopedia of Medical Devices and Instrumentation, Second Edition*, J. G. Webster, Ed., ed: John Wiley &Sons, Inc., pp. 120-166, 2006.

[23] J. N. Israelachvili, "Intermolecular and Surface Forces," *2nd ed., Academic, San Diego,* 1992.

[24] S. Cai and B. Bhushan, "Three-Dimensional Dry/Wet Contact Analysis of Multilayered Elastic/Plastic Solids with Rough Surfaces," *Transactions of the ASME,* vol. 128, pp. 18-30, 2006.

[25] B. Bhushan, "Adhesion and Stiction: Mechanisms, Measurement Techniques, and Methods for Reduction," *Journal of Vaccum Science & Technology B,* vol. 21(6), pp. 2262-2296, 2003.

[26] X. Tian and B. Bhushan, "The micro-meniscus effect of a thin liquid film on the static friction of rough surface contact," *Journal of Physics D: Applied Physics,* vol. 29, pp. 163-178, 1996.

[27] A. B. Usakli, "Improvement of EEG Signal Acquisition: An Electrical Aspect for State of the Art of Front End," *Hindawi Publishing Corporation - Computational Intelligence and Neuroscience,* p. 7 pages, 2010.

[28] M. Braunovic, V. V. Konchits, and N. K. Myshkin, *Electrical contacts: Fundamentals, Applications and Technology*, 2007.

ACTA Press

An Electro-Mechanical Contact Formulation for Dry/Wet Electrode-Scalp Interfaces in an EEG Headset

Vangu Kitoko, Tuan N. Nguyen, and Hung T. Nguyen

Keywords

Bristle electrode, Wearable EEG headset, Skin roughness, scalp

Abstract

The process of generating an initial prototype for a new dry electrode wearable EEG headset system design can be time and resource intensive. The ability to predict the mechanical and electrical characteristics of this recording device could lead to major cost savings in this process. Since the skin surface roughness has a deep impact on the decrease of brain electric contact conductance (or the increase of the contact impedance) when electrode with bristles contact scalp skin, the estimation of electric conductance across rough dry and wet boundaries is a challenging task in the designing optimization of the wearable EEG headset system. In this contribution, the contact mechanism to predict the electrical conductance of scalp skin pressed against the electrode is considered as the electrical connection by the mechanical contact. For mechanical contact analysis, a new normal force-displacement approach based on the micro-mechanical studies is developed for analyse of the non-linear electrode-skin contact interface problem with “high contact precision”. For the electrical contact conductance modelling, in this paper, we have extended the Pohrt and Popov model by including the effects of conductive gel. An experiment is developed and carried-out to validate the interfacial contact impedance model.

Important Links:

- DOI: 10.2316/P.2013.791-141
- *From Proceeding* (791) Biomedical Engineering - 2013

Go Back




IASTED
The International Association of Science and Technology for Development

Call for Papers

BEST PAPER AWARDS

Winners will be selected for the following conference awards to recognize outstanding research works presented at BioMed 2013.

- Best Conference Paper Award
- Best Student Paper Award

For more information, visit:
http://www.iasted.org/conferences/cfp-791.html#award.

TUTORIALS

Submission

Proposals for three-hour tutorials must be submitted online by **September 17, 2012**. Submit tutorial proposals via the following web site address:
http://www.iasted.org/conferences/tutorialsubmit-791.html.

Proposal Format

A tutorial proposal should clearly indicate:

- The topic
- Background knowledge expected of the participants
- Objectives
- Time allocations for the major course topics
- The qualifications of the instructor(s)

JOURNALS

Papers submitted to this conference that have been revised to include new results and offer an unique contribution may be considered for possible publication in the International Journal of Computational Bioscience. For additional information about the submission of papers, please visit: **www.actapress.com/SubmissionInfo.aspx**.

INDEXING

The proceedings will be sent for indexing in the following:

- EI Compendex
- Inspec
- Google Scholar
- Scopus

CONCURRENT CONFERENCES

BioMed 2013 will be held in conjunction with the IASTED International Conferences on:

- Web-based Education (WBE 2013)
- Artificial Intelligence and Applications (AIA 2013)
- Modelling, Identification and Control (MIC 2013)
- Parallel and Distributed Computing and Networks (PDCN 2013)
- Software Engineering (SE 2013)
- Computer Graphics and Imaging (CGIM 2013)
- Signal Processing, Pattern Recognition and Applications (SPPRA 2013)

INTERNATIONAL PROGRAM COMMITTEE

** At Time of Printing*

D. Abasolo – UK
A. Baca – Austria
E. Blangino – Argentina
N. Botros – USA
M. Brandl – Austria
K. Camilleri – Malta
K.S. Cheng – Taiwan
A. Choubey – USA
K. Cieslicki – Poland
O. Ciobanu – Romania
D. Coca – UK
A. Fenster – Canada
S. Finkelstein – USA
J. Fisher – UK
J.M. Fonseca – Portugal
T. Fukuda – Japan
J. Hong – Korea
R. Hornero – Spain
Y.J. Hu – Taiwan
I. Ibraheem – Syria
H. Jiang – USA
R. Kiss – Hungary
G. Kontaxakis – Spain
B.D. Kuban – USA
J.J. Lee – Taiwan
N. Lovell – Australia
K.G. Neoh – Singapore
D. Ng – Australia
A.G. Patil – India
T. Podder – USA
J. Ren – UK
R. Ron-Angevin – Spain
A. Rosa – Portugal
C. Ruggiero – Italy
V.F. Ruiz – UK
F.K. Schneider – Brazil
J.S. Shieh – Taiwan
D.M. Simpson – UK
A. Swierniak – Poland
D.Y. Tsai – Japan
M. Tsuzuki – Brazil
T. Webster – USA

IMPORTANT DEADLINES

Submissions due	September 17, 2012
Notification of acceptance	November 1, 2012
Final manuscripts due	November 15, 2012
Registration and full payment	December 3, 2012

CONTACT US

IASTED Secretariat – BioMed 2013
B6, Suite 101, 2509 Dieppe Avenue SW
Calgary, AB, Canada T3E 7J9
Tel: 403-288-1195 Fax: 403-247-6851
calgary@iasted.org
www.iasted.org/conferences/cfp-791.html


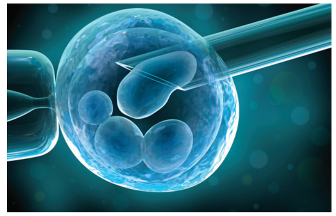

The 10th IASTED International Conference on

Biomedical Engineering (BioMed 2013)

Technical Co-Sponsor

IEEE EMB

February 13 – 15, 2013
Innsbruck, Austria

Biomedical Engineering

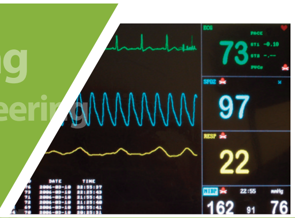
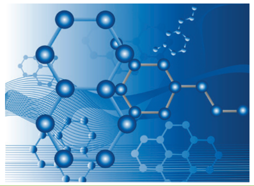

SPONSOR
The International Association of Science and Technology for Development (IASTED)

TECHNICAL CO-SPONSOR
IEEE Engineering in Medicine and Biology Society

CONFERENCE CHAIR
Prof. Aldo R. Boccaccini – University of Erlangen-Nuremberg, Germany

KEYNOTE SPEAKER
Prof. C. James Kirkpatrick – Johannes Gutenberg University, Germany

INVITED SPEAKER
Prof. Sian E. Harding – Imperial College London, UK

SPECIAL SESSION ORGANIZERS
Dr. Rainer Detsch – University of Erlangen-Nuremberg, Germany
Prof. Enrica Verne – Politecnico di Torino, Italy
Prof. Issa Ibraheem – Damascus University, Syria
Dr. Marie-Noëlle Giraud – University of Fribourg, Switzerland

TUTORIAL PRESENTER
Prof. Christian Hellmich – Vienna University of Technology, Austria

PURPOSE
With the aid of engineering and information technology, biomedical engineering has emerged as a high-tech field, generating innovation in such areas as medical imaging, bioinformatics, MEMS, sensors and nanotechnology, new biomaterials, regenerative medicine and tissue engineering scaffolds, medical robotics, and neurobiology. Scientists and engineers in this field work towards such advances as developing artificial organs that mimic natural human organs, cell based therapies, optimising bioresponsive materials and implants with enhanced biological activity and drug delivery ability, conducting telemedicine, performing surgeries with robots, creating laboratory-on-a-chip approaches, and controlling robots through natural animal brain matter.

IASTED's 10th International Conference on Biomedical Engineering will bring together leading experts in the key interdisciplinary fields of biomedical engineering.

LOCATION
Innsbruck has always been valued as a European treasure by monarchs and civilians alike, and today remains a tourist favourite for its charm, history, and natural beauty. Scenically positioned between impressive mountain ranges and the Inn River, and several lakes nearby as well, the town is ideal for winter sports: skiing and snowboarding hills are right outside the door. Come and visit Innsbruck, where you can explore or just relax in a charming mountain village.

SCOPE
The topics to be covered include, but are not limited to:

Health Care Technology
- Clinical Assessment and Patient Diagnosis
- Artificial Organs
- Computer-aided Surgery
- Electrotherapy
- Health Care Information Systems
- Implant Technology
- Patient Monitoring
- Prosthetics and Orthotics
- Radiotherapy
- Rehabilitation Engineering
- Telemedicine

Medical Devices, Biomedical Materials, Measurement and Instrumentation
- Biomechanics
- Biosensors and Transducers
- Data and Signal Acquisition
- Electronic Medical Devices
- Intelligent Instrumentation
- Lasers and Optical Systems
- Measurement and Instrumentation
- Microtechnology and BioMEMS
- Noninvasive Measurement
- Reliability and Failure

Medical Imaging, Image and Signal Processing
- Computed Tomography
- Data Representation and Visualization
- Integrated Medical Image Analysis
- Magnetic Resonance Imaging
- Nuclear Medicine
- Medical Data Storage and Compression
- Medical Image Processing
- Optical Imaging
- Biomedical Signal Processing
- Ultrasound Imaging

Modelling, Simulation, Systems and Control
- Biomedical Computing
- Electromagnetic Field Simulation
- Hemodynamics
- Sports and Ergonomics Simulation
- Surgery Simulation and Simulators
- Virtual Reality

Molecular Bioengineering
- Labs-on-Chips
- Bio-Nanotechnology
- Tissue Engineering
- Drug Delivery and Pharmacokinetics
- Bioinformatics

Innsbruck


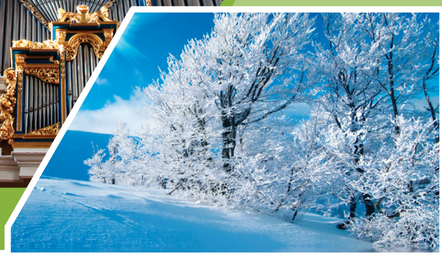

SUBMISSION
Submit your paper via our website at: **www.iasted.org/conferences/submit-791.html**. All submissions should be in Adobe Acrobat (.PDF) format.

The IASTED Secretariat must receive your paper by **September 17, 2012**. Receipt of paper submission will be confirmed by email.

Initial Paper Requirements
Initial paper submissions should be **full papers.** Papers of up to 8 pages in length are included in the conference registration fee. An extra charge will apply for every additional page for papers longer than 8 pages. Authors are responsible for having their papers checked for style, grammar and originality before submitting to IASTED.

Formatting instructions for initial papers are available at **www.iasted.org/formatting-initial-page.html**.

Reviewing
All papers submitted to this conference will be double-blind peer reviewed by at least two members of the International Program Committee and related technical committees. Acceptance will be based primarily on originality, significance, technical soundness, presentation, and references. The conference chair makes the final decision on the acceptance or rejection of the paper.

Acceptance and Registration
Notification of acceptance will be sent via email by **November 1, 2012**. Final manuscripts are due by **November 15, 2012**. Registration and final payment are due by **December 3, 2012**. Late registration fees or paper submissions will result in the papers being excluded from the conference proceedings. Only one paper of up to eight pages is included in the regular registration fee. There will be an added charge for extra pages and additional papers.

SPECIAL SESSION PAPER SUBMISSIONS
Authors can also submit a paper to the following special sessions by **September 17, 2012**:

"Rapid Prototyping and Cell Printing for Regenerative Medicine"
http://www.iasted.org/conferences/session1-791.html

"Biomedical Coatings"
http://www.iasted.org/conferences/session2-791.html

"Spectral Imaging (imaging spectroscopy) for Medical Diagnosis and Pharmaceutical Applications"
http://www.iasted.org/conferences/session3-791.html

"Cardiac Regeneration Approaches"
http://www.iasted.org/conferences/session4-791.html

PRELIMINARY CONFERENCE PROGRAM

The 10th IASTED International Conference on Biomedical Engineering (BioMed 2013)
February 13 - 15, 2013
Innsbruck, Austria

LOCATION
Congress und Messe Innsbruck GmbH
Rennweg 3, 6020 Innsbruck
Austria

BIOMEDICAL ENGINEERING (BioMed 2013)

SPONSOR
The International Association of Science and Technology for Development (IASTED)

TECHNICAL CO-SPONSOR

IEEE Engineering in Medicine and Biology Society

CONFERENCE CHAIR
Prof. Aldo R. Boccaccini - University of Erlangen-Nuremberg, Germany

KEYNOTE SPEAKER
Prof. C. James Kirkpatrick - Johannes Gutenberg University, Germany

INVITED SPEAKER
Prof. Sian E. Harding - Imperial College London, UK

TUTORIAL SESSION
Prof. Christian Hellmich - Vienna University of Technology, Austria

SPECIAL SESSIONS ORGANIZERS
Dr. Rainer Detsch - University of Erlangen-Nuremberg, Germany
Prof. Enrica Verne - Politecnico di Torino, Italy
Prof. Issa Ibraheem - Damascus University, Syria
Dr. Marie-Noëlle Giraud - University of Fribourg, Switzerland
Prof. Christian Hellmich - Vienna University of Technology, Austria
Prof. Hans Van Oosterwyck - KU Leuven, Belgium
Prof. Nenad Filipovic - University of Kragujevac, Serbia
Dr. Stefan Scheiner - Vienna University of Technology, Austria

INTERNATIONAL PROGRAM COMMITTEE
D. Abasolo – University of Surrey, UK
A. Baca – University of Vienna, Austria
E. Blangino – University of Buenos Aires, Argentina
N. Botros – Southern Illinois University at Carbondale, USA
M. Brandl – Danube University Krems, Austria
K. Camilleri – University of Malta, Malta
K. S. Cheng – National Cheng Kung University, Taiwan
A. Choubey – Palmaz Scientific, Inc., USA
K. Cieslicki – Warsaw University of Technology, Poland
O. Ciobanu – Gr.T.Popa University of Medicine and Pharmacy, Romania
D. Coca – University of Sheffield , UK
A. Fenster – The University of Western Ontario, Canada
S. Finkelstein – University of Minnesota, USA
J. Fisher – University of Leeds, UK
J. M. Fonseca – UNINOVA, Portugal
T. Fukuda – Nagoya University, Japan
K. Höller – Friedrich-Alexander-Universitaet Erlangen-Nürnberg, Germany
J. Hong – Korea University, Korea
J. Hornegger – Friedrich-Alexander-Universität Erlangen-Nürnberg, Germany
R. Hornero – University of Valladolid, Spain
Y. J. Hu – National Chiao Tung University, Taiwan
I. Ibraheem – Damascus University, Syria
H. Jiang – University of Florida, USA
R. Kiss – Budapest University of Technology and Economics, Hungary
G. Kontaxakis – Universidad Politécnica de Madrid, Spain
B. D. Kuban – Cleveland Clinic Foundation, USA
J. J. Lee – National Yang Ming University, Taiwan
N. Lovell – University of New South Wales, Australia
K. G. Neoh – National University of Singapore, Singapore
D. Ng – National ICT Australia, Australia
A. G. Patil – S.B.M. Polytechnic, India
T. Podder – University Hospitals Case Medical Center, USA
J. Ren – Liverpool John Moores University, UK
R. Ron-Angevin – University of Malaga, Spain
A. Rosa – IST - Technical University of Lisbon, Portugal
C. Ruggiero – University of Genova, Italy
V. F. Ruiz – University of Reading, UK
A. Santos – Universidad Politecnica de Madrid, Spain

Wednesday, February 13, 2013

07:30 – REGISTRATION
Location: Diesner Foyer

08:00 – 08:30 BioMed WELCOME ADDRESS
Location: Hall Strassburg

08:30 – BioMed SESSION 1 - BIOMEDICAL SIGNAL PROCESSING SYSTEMS AND CONTROL I
Chairs: TBA
Location: Hall Strassburg

791-156
Automated Extraction of Principal Components of Non-Structural Protein 1 from SERS Spectrum
Afaf R. Mohd Radzol, Yoot K. Lee, Wahidah Mansor, and Faizal Mohd Twon Tawi (Malaysia)

791-159
Changes in Bilateral Phase Synchronization in Parkinsonian Tremor Related to Amplitude Difference
Sang Kyong Kim, Hyo Seon Jeon, Han Byul Kim, Ko Keun Kim, Beom Seok Jeon, and Kwang Suk Park (Korea)

791-141
An Electro-Mechanical Contact Formulation for Dry/Wet Electrode-Scalp Interfaces in an EEG Headset
Vangu Kitoko, Tuan N. Nguyen, and Hung T. Nguyen (Australia)

791-100
A Time-Series Pre-Processing Methodology for Biosignal Classification using Statistical Feature Extraction
Simon Fong (Australia), Kun Lan, Paul Sun (PR China), Sabah Mohammed, and Jinan Fiaidhi (Canada)

791-077
Wrist Pulse Signal Acquisition System Design
Bhaskar Thakkar and Anoop L. Vyas (India)

791-149
Computer Models for Gait Identification and Analysis using Autonomous System for Control and Monitoring
Ivanka P. Veneva (Bulgaria)

791-126
Knowledge Discovery and Knowledge Reuse in Clinical Information Systems
Jon D. Patrick (Australia), Leila Safari (Iran), and Yuzhong Cheng (PR China)

791-158
Cauchy Wavelet-based Mechanomyographic Analysis for Muscle Contraction Evoked by FES in a Spinal Cord Injured Person
Eddy Krueger, Eduardo M. Scheeren, André E. Lazarretti, Guilherme N. Nogueira-Neto, Vera L.S.N. Button, and Percy Nohama (Brazil)

791-174
Wavelet Filter Proposal to Attenuate the Background Activity and High Frequencies in EEG Signals
Geovani R. Scolaro, Christine F. Boos, and Fernando M. Azevedo (Brazil)

10:30 – 11:00 COFFEE BREAK
Location: Diesner Foyer

11:00 – BioMed SESSION 1 CONTINUED
Location: Hall Strassburg

12:00 – LUNCH BREAK
Self-Catered

14:00 – BioMed SESSION 2 - MEDICAL IMAGING MRI ROBOTICS MONITORING I
Chairs: TBA
Location: Hall Strassburg

791-026
Assessment of Asymmetry in Dermoscopic Colour Images of Pigmented Skin Lesions
Joanna Jaworek-Korjakowska and Ryszard Tadeusiewicz (Poland)

791-081
Automated Processing Pipeline for Texture Analysis of Childhood Brain Tumours based on Multimodal Magnetic Resonance Imaging
Suchada Tantisatirapong, Nigel P. Davies, Lawrence Abernethy, Dorothee P. Auer, Chris A. Clark, Richard Grundy, Tim Jaspan, Darren Hargrave, Lesley MacPherson, Martin O. Leach, Geoff S. Payne, Barry L. Pizer, Andrew C. Peet, and Theodoros N. Arvanitis (UK)

791-105
Evaluation of CT-based 3D-Printed Colon Models for Surgical Operation Planning
Nikita Shevchenko, Sonja Gillen, Hubertus Feußner, and Tim C. Lüth (Germany)

791-128
Analysis of Right Ventricular Remodeling using Curvature Histogram Comparison
Soo-Kng Teo, Si-Yong Yeo, Chi Wan Lim, Liang Zhong, Ru-San Tan, and Yi Su (Singapore)